Journal of Chemical Engineering & Process Technology

Seifollahzadeh and Aminian, J Chem Eng Process Technol 2014, 5:2
DOI: 10.4172/2157-7048.1000185

Research Article Open Access

Simulation and Study of the Effect of Pressure Oscillations on Linear Combustion Instability in a Double Base Solid Rocket Motor

Ali Seifollahzadeh and Ali Aminian*

Department of Chemistry and Chemical Engineering, MAUT, Tehran, Iran

Abstract

The combustion instability remained as a problem during solid rocket motors progress. In this study, combustion instability of a double base solid rocket motor was estimated wherein acoustical and erosive burning was considered. The ballistic parameters of the solid rocket motor were presented and the results were compared with simulations, which show a good agreement. The result shows that specific impulse of the solid propellant rocket motor was obtained 211 s and the maximum pressure of the combustion chamber reaches 13.8 MPa. Combustion instability analysis indicates that the motor became unstable after 0.5 s.

Keywords: Combustion instability; Double base solid propellant; Internal ballistic; Erosive burning; Acoustic modes

Introduction

Combustion instability is referred to the pressure oscillations duo to unsteady burning rate in the combustion chambers. Rocket motor combustion instability is caused by pressure fluctuations and acoustic resonances in the combustion chamber, which may reduce engine performance, induce structural vibration, increase wall heat transfer, and possibly lead to catastrophic failure in combustion chamber.

Current remedy for reducing instabilities occurring in solid rocket motors is either by changing propellant composition, or improving the design of the combustion chambers. Non-steady burning and combustion instabilities appearing in solid propellants have been investigated extensively both theoretically and experimentally.

Due to considerable cost, time and difficulties encountered during motor firing tests, cold flow experiments and numerical simulations can be used to study the type of flow field in solid rocket motors [1,2]. The comparison between the results of such simulations and experimental findings help to better understanding flow pattern in combustion chambers and acquire useful information on combustion instability driven processes.

One important elements of the combustion instability are obstacles and corners in the combustion chamber cavity, which are leads to the vortex generation. Flandro and Jacobs [3] was first made acoustic mode excitation by vortex shedding in solid propellant rocket motors. The effect of nozzle cavity on suppression of vortex shedding was clearly stated by Fabignon et al. [4].

The acoustic energy lost as a result of energy transfer from acoustic pressure oscillations to the vortical gas waves produces axial gas motion known as flow turning. Flandro [5] has shown that for cylindrical grain covering 80% of the total chamber length the flow turning growth rates were -1, -0.25, +0.25 for first, second, and third axial modes, respectively. Also, the inclusion of flow turning correction term in growth rate calculations make better agreement between exact values and predicted ones.

Another important feature of the combustion instability is the effects of Combustion stability additives like zirconium carbide (ZrC), aluminum oxide ($A1_2O_3$), and zirconium ortho-silicate ($ZrSiO_4$) on suppressing combustion instability in solid propellant rocket motors. The additives appear to have effects on changing the response behavior of the propellant. In addition, high specific impulse in a solid propellant motor is generally achieved by metals. Metal combustion increases the temperature and the pressure inside the chamber [6].

The experiments show that propellants with stabilizing additives have no instability under different pulses and mild operating conditions. Higher pressure solid rocket motors are more susceptible to pulsed instability at lower pulse amplitudes. The thermal and momentum relaxation times of particles play an important role in dictating the two-phase flow interactions with oscillatory motor internal flows [7]. Small particles with a wide range of particle distribution have higher relaxation time and usually exert greater influence on the dispersion of acoustic energies. In general, the effect of energy exchange tends to be more profound for low-frequency acoustic oscillations [8].

Aluminum combustion occurs close to the burning surface, implying that this have a little impact on the oscillatory behavior. On the other hand, turbulence has a little influence on the acoustic wave oscillation. The turbulent-flow-induced particle dispersion phenomena have considerable effect on damping out the turbulent region by the turbulence-induced eddy viscosity [9].

In order to study the effects of grain configurations on combustion instability, a series of small test motor firings with various grain configurations was used [10]. Their tests showed that combination of STAR-circular perforation configuration offers a great stability margin during entire motor firing.

Since, in a solid rocket motor, pressure is spanned between 5-25 MPa and temperature varies between 2300-3600 K, real measurements in a practical motors are impossible, using only research burners can obtain the desire parameters with changing the operating conditions.

In order to predict the stability characteristics of the solid propellant

***Corresponding author:** Ali Aminian, Department of Chemistry and Chemical Engineering, MAUT, Tehran, Iran, Tel/Fax: +9822945143; E-mail: ali_aminian@ymail.com

Received December 19, 2013; **Accepted** January 28, 2014; **Published** January 30, 2014

Citation: Seifollahzadeh A, Aminian A (2014) Simulation and Study of the Effect of Pressure Oscillations on Linear Combustion Instability in a Double Base Solid Rocket Motor. J Chem Eng Process Technol 5: 185. doi: 10.4172/2157-7048.1000185

rocket motor combustion, it is require defining acoustic boundary conditions at the propellant surface, namely how the instantaneous propellant burning rate responds to pressure or cross flow velocity fluctuations.

The pressure perturbation generates perturbations in the burning rate, since the burning rate of the solid propellants are pressure dependent, and consequently there are perturbations in gas flow from burning surface. Whether or not the acoustic wave is amplified upon reflection depends on the nature of the gas flow/pressure connection. To include this effect it is required to solve the unsteady gas flow equations. An effective model combines the effects of the unsteady flow, the transient combustion process, and the boundary conditions.

The objective of this work is to utilize a simulation capability that can be used to further investigate the flow field generated through the entire combustion chamber and analyzing the combustion instability of the concerned solid rocket motor. To further proceed, two major models have been implemented: 1) the chamber pressure was assumed to be uniform in the entire chamber and the time evolution of pressure history was calculated. Other ballistic characteristics of the solid rocket motor were also obtained including thrust and specific impulse. Furthermore, combustion instability analysis was performed during the burning out of the propellant, 2) transient combustion for studying chamber flow dynamics.

Dynamic Combustion Models

This work uses the Lax-Wandrroff technique to solve for the 1-D flow field in a double base solid propellant rocket motor. In this study, non-aluminized double base solid propellant have been the primary interest, the following simplifying assumptions were made: (1) the solid propellant combustion process can be described in a single spatial dimension, (2) the unburned propellant is homogeneous, incompressible, and inert, (3) the solid is converted into gas by a global pyrolysis reaction which occurs at an infinitesimally thin interface, and (4) the gas-phase flame is quasi-steady and remains anchored to the interface.

Therefore, the 1-D inviscid flow equation with source terms to incorporate the mass injection from the burning propellant was used for modeling the transient combustion of the solid propellant rocket motor [11]:

$$\frac{\partial U}{\partial t}+\frac{\partial F}{\partial x}=S \quad (1)$$

Where

$$U=\left[\rho,\rho u,\rho e_t A\right]$$

$$F=\left[\rho u A,(\rho u^2+p)A,(\rho e_t+p)Au\right]$$

$$S=\left[\rho_p r_b P, p\frac{\partial A}{\partial x}-\rho_p r_b P u, \rho_p r_b P(h_c+\frac{1}{2}u_f^2)\right]$$

It was assumed that the flow in the combustion chamber is Quasi-1D unsteady inviscid flow, in which ρ, u, p, A, ρ_p, r_b, u_f, h_c and P are gas density, velocity, pressure, port area, propellant density, mass burning rate, injection velocity of combustion products, heat of combustion, and perimeter of solid propellant, respectively. Total energy in the combustion chamber and injection velocity of combustion products are defined as

$$e_t=\frac{p}{(\gamma-1)\rho}+\frac{u^2}{2} \quad (2)$$

$$u_f=\frac{\rho_p r_b}{\rho} \quad (3)$$

$$\dot{m}_g=S_b\rho_p r \quad (4)$$

For 1-D simulations, numerical calculations were performed to obtain the axial pressure, velocity, temperature, and other internal flow parameters using Eq 1-3. Mass injection rate is calculated by the product of the burning rate (from burning rate model), burning area, and solid propellant density [see Eq. (4)]. The boundary conditions are u = 0, since the head end of the motor is inert and initial p is the medium pressure. Because of numerical stability considerations, the time step is evaluated using the Courant-Friedrichs-Lewy (CFL) number and spatial grid size *h* defined as below,

$$dt=\frac{CFL\times h}{max(a)} \quad (5)$$

The CFL number must be less than unity and *a* is the speed of sound.

In order to guarantee stability of the solution, another term named as artificial viscosity is added to numerical solution of partial differential equations (1).

Major ingredients of the propellant are 55.25% NC, 33.84% NG. The global pressure-dependent burning rate model was used to predict the pressure variations on the burning rate for quasi-steady state simulation as [12]

$$r_b=0.01372(P)^{0.2276} \quad (6)$$

Where P in Mpa and the unit of r_b is m/s.

The erosive burning contribution to the over-all burning rate can be written as follows:

$$r=r_b+r_e \quad (7)$$

Since two burning rates are additive, the pressure-dependent burning rate (r_b) calculated from mean chamber pressure, while erosive burning term r_e depends on the gas flux, flame and surface temperatures. Erosive burning rate is written as [13,14]

$$r_e=\alpha\, G_g^{0.8}exp\left(-\beta r_b\rho_p/G_g\right)/L^{0.2}$$
$$\alpha=\frac{0.028c_{p_g}\mu_g^{0.2}pr_g^{-0.67}}{\rho_p C_{p_s}}\left(\frac{T_c-T_s}{T_s-T_0}\right) \quad (8)$$

Where β is an empirical constant about 53 [13], c_{p_g} and c_{p_s} are specific heats of gas and solid propellant respectively, μ_g gas viscosity, p_g Prantle number for the gas phase, T_s surface temperature, T_0 initial grain temperature, and G_g is mass flux of the combustion gases leaving the burning surface.

The double-base solid propellant density, adiabatic flame temperature, grain length, chamber radius, web thickness, nozzle throat

Citation: Seifollahzadeh A, Aminian A (2014) Simulation and Study of the Effect of Pressure Oscillations on Linear Combustion Instability in a Double Base Solid Rocket Motor. J Chem Eng Process Technol 5: 185. doi: 10.4172/2157-7048.1000185

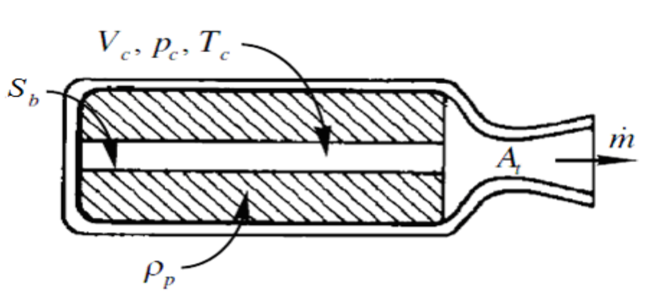

Figure 1: Schematic of the solid propellant rocket motor.

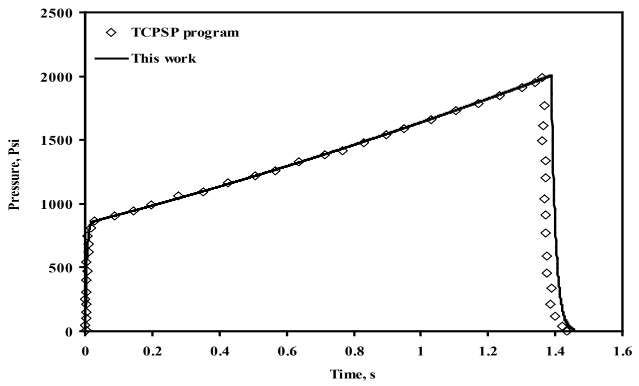

Figure 2: Comparison between the calculated pressures of this work and TCPSP program [12].

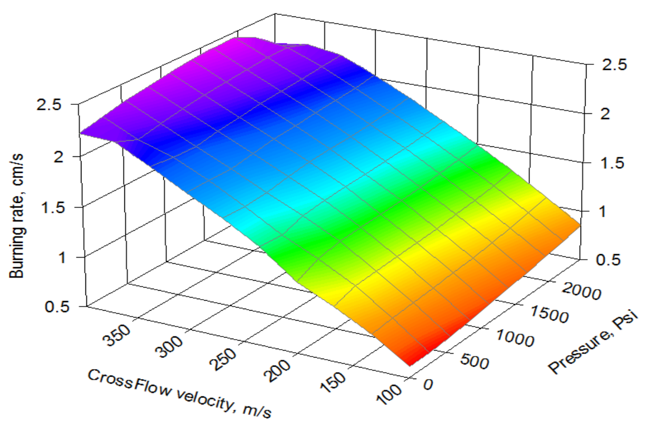

Figure 3: 3-D plot of the effect of pressure and cross flow velocity on the burning rate.

diameter, and outer diameter of the nozzle are 1600 kg/m^3, 2351 K, 0.52 m, 120 mm, 22 mm, 24.4 mm, 79.5 mm, respectively. Figure 1 shows the schematic representation of the solid rocket motor.

The thrust for a rocket motor is

$F(t) = P_c(t) A_t C_F(t)$ (9)

Where the thrust coefficient, C_F, can be expressed in terms of chamber pressure and exit pressure [12]

$$C_F(t) = \eta_F \sqrt{2\frac{\gamma^2}{\gamma-1}\left(\frac{2}{\gamma+1}\right)^{(\gamma+1)/(\gamma-1)}\left[1-\left(\frac{P_e}{P_c}\right)^{(\gamma-1)/\gamma}\right]} + \frac{P_e - P_{atm}}{P_c}\left(\frac{A_e}{A_t}\right) \quad (10)$$

The total impulse of the solid rocket motor is obtained by integration of thrust over burning time

$$I = \int_0^t F(t)\,dt \quad (11)$$

For uniform spatial but time varying pressure distribution simulations along the chamber axis, the mass balance equation is used to calculate the chamber pressure. The chamber pressure is assumed to be uniform throughout the rocket chamber; therefore, the burning rate is uniform as well. With the above assumptions described above, the chamber pressure is solved from mass balance equation:

$$\frac{\partial}{\partial t}\int_{V_c} \rho dV + \oint_{S_c} \rho u.dS = 0 \quad (12)$$

The second term in eq 12 is mass of the gas in every instantaneous time in the combustion chamber. We can obtain the pressure-time relation from eq. 12 as follows

$$P_c(t) = \left[\left(P_{atm}^{1-n} - \frac{a(\rho-\rho_p)s_b}{C_D A_t}\right)\exp\left(\frac{(n-1)RT_c C_D A_t t}{V_c}\right) + \frac{a\rho_p S_b}{C_D A_t}\right]^{1/1-n} \quad (13)$$

Where P_c, T_c, V_c, S_b, A_t, C_D, n, and t are chamber pressure, temperature, volume burning area, throat area, nozzle discharge coefficient, pressure exponent, and time, respectively.

Results and Discussion

The solid rocket motor uses non-metalized double base propellant. Figure 2 shows the comparison between the calculated pressures and simulated by TCPSP program [12] for the quasi-steady state model. As can be seen from Figure 2, there is a good agreement between the calculated pressures and simulated by TCPSP program for quasi-steady state model. Solid rocket motor has no pressure spike addressing erosive burning normal to the burning surface can be neglected in this motor. The characteristic length of the solid rocket motor L^* (=V/A_t) start with a value of approximately 115 cm.

As shown in Figure 2, there is no induce bulk-mode or L^* instability in the solid rocket motor under consideration. Figure 3 shows the 3-D plot of the effect of pressure and cross flow velocity of combustion gases released from burning surface on the burning rate. The burning rate increases almost linearly with cross flow velocity mainly due to enhanced heat transfer by turbulence in the fizz zone [11].

Figure 4 shows the thrust vs. time for double base solid rocket motor.

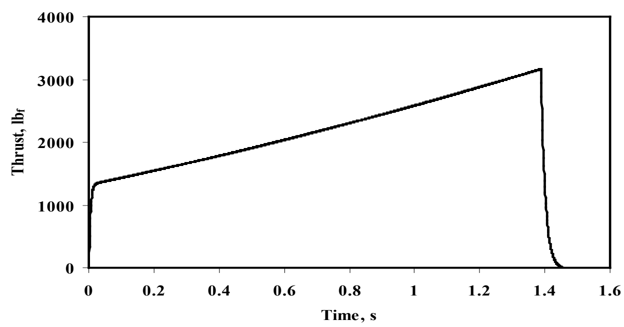

Figure 4: Calculated thrust of the solid rocket motor.

Citation: Seifollahzadeh A, Aminian A (2014) Simulation and Study of the Effect of Pressure Oscillations on Linear Combustion Instability in a Double Base Solid Rocket Motor. J Chem Eng Process Technol 5: 185. doi: 10.4172/2157-7048.1000185

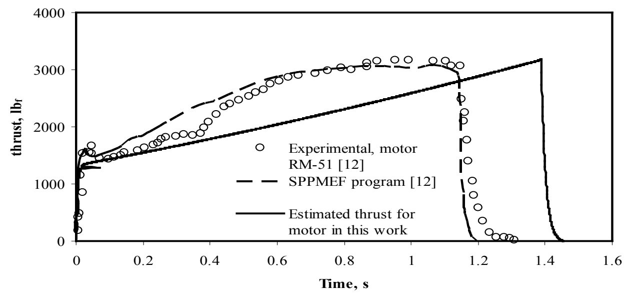

Figure 5: Comparison between the thrust vs. time for the solid rocket motor of this work and the thrust obtained for RM-51 using SPPMEF program [12].

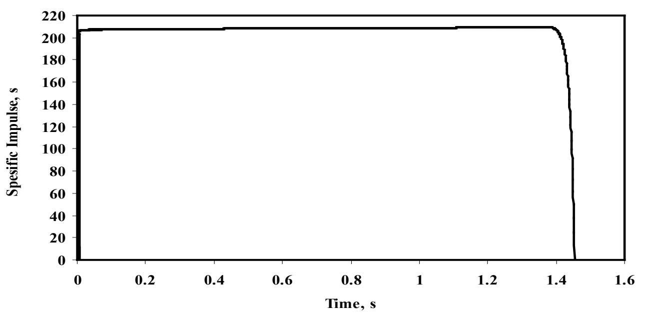

Figure 6: Variation of specific impulse vs. time for the circular perforation grain.

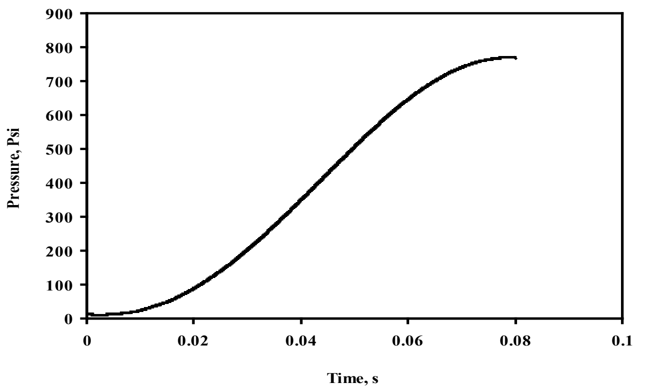

Figure 7: Transient combustion of the solid rocket motor.

As can be seen from Figure 4, the thrust of the solid rocket motor with circular perforation grain was progressive, reaches its maximum during the end of the burning time.

Comparison between the calculated thrust of the solid rocket motor in this work and the thrust obtained from solid rocket motor RM51 wit experimental thrust data for RM51 is shown in Figure 5. As in Figure 5, there is a good agreement between the thrust of this work and the calculated thrust in Ref [12].

A parameter that is used to identify the energy efficiency of propellant combustion named as Specific impulse. This parameter represents the performance of a rocket motor during its operating flight. The plot of specific impulse versus time is depicted in Figure 6.

The specific impulse of the double base solid rocket motor was obtained 211 s. currently, the performance of the solid rocket motors is improved by adding to the propellant ingredients some metal powders and/or ammonium percholorate [6].

The result of the transient combustion simulation for the pressure can be seen in Figure 7. It is interesting to note that after ignition transients have stabilized, the solid rocket motor pressure follows the trend of the motor's total burning surface area [15]. As mentioned before, the optimum grain configuration comprises a star follows a circular perforation, because erosive burning is expected to be most significant at the beginning of the burn. There is a balance between the enhanced burning rate due to erosive burning and increased burning area due to star shape of the grain at the head end.

In order to analyze the stability of the solid rocket motor, linear contributions of combustion process, flow turning, and nozzle damping were considered. Since pressure amplitudes are function of mean chamber pressure, overall growth constant have the general form

$\alpha_T = \alpha_C + \alpha_F + \alpha_N$

The amplitude of the oscillations increases with time when $\alpha_T > 0$ and therefore is unstable. If $\alpha_T < 0$, the amplitude decreases with time and the oscillations are stable. Assuming linear combustion instability and one dimensional flow in the combustor, it is possible to write the growth rates of combustion α_C, flow turning α_F, and nozzle α_N as follows

$$\alpha_c = \frac{\bar{a}}{2}\bar{M}_b . R_b^{(r)} \left[\frac{\iint \psi_n^2 dS_b}{\int_0^L \psi_n^2 S_c dz} \right] \tag{14}$$

$$\alpha_F = \frac{\bar{M}_b}{2E_1^2} . \iint_{S_b} [\cos(2k_1 z)] dS_b \tag{15}$$

$$\alpha_{Nozzle} \equiv \alpha_N = -\frac{1}{2E_1^2}\left[\left(\gamma \frac{\hat{u}^{(r)}}{\hat{\eta}_1}\psi_1 + \bar{u}\psi_1^2\right) S_c\right]_{z=L} \approx -\frac{\bar{a}}{2}\left(\frac{\gamma+1}{2}\right)\bar{M}_n \left[\frac{\iint \psi_n^2 dS_n}{\int_0^L \psi_n^2 S_c dz} \right] \tag{16}$$

Where $E_1^2 = \int_0^L \psi_1^2 S_c dz = S_c \frac{L}{2}$ and $\psi_l^2 = \cos^2(k_l L)_{z=L} = 1, k_l = l\pi / L$, $\bar{M}_n$ =Mach number flow at the nozzle entrance, $\bar{M}_b$ = the Mach number of flow at propellant surface, S_n = Nozzle inlet area, S_b = burning surface area, S_c = cross sectional area, $R_b^{(r)}$ = real part of propellant response function, and $\bar{a}$ is the speed of sound.

The common response function that was used is Denison and

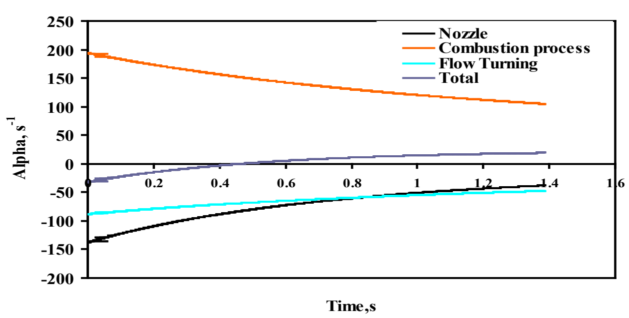

Figure 8: Predicted stability boundary for the solid propellant rocket motor.

Baum model based on flame model with zero heat flux absorption in depth of solid:

$$R_b = \frac{nAB + n_s(\lambda - 1)}{\lambda + \frac{A}{\lambda} - (1+A) + AB - \frac{Q_r A(\lambda - 1)}{\lambda(\beta + \lambda - 1)}} \tag{17}$$

For double base propellants Arrhenius surface pyrolysis law (which carries with it the condition n_s=0) can be applied.

With the assumption of negligible radiant flux, it follows that $Q_r \rightarrow 0$, response function of the double base propellant under consideration can be obtained with λ that satisfies the equation

$$\lambda(\lambda-1)= i\Omega \tag{18}$$

$$\Omega = \frac{k_p \rho_s \omega}{\bar{m}^2 C} \tag{19}$$

Where $\overline{m}$ is the average mass flux of combustion gases. The solution of the eq. (17) with real part λ_r and imaginary part λ_i are

$$\lambda_r = \frac{1}{2}\left\{1 + \left[\frac{1}{\sqrt{2}}\right]\left[\left(1+16\Omega^2\right)^{1/2} + 1\right]^{1/2}\right\} \tag{20}$$

$$\lambda_i = \left[\frac{1}{2\sqrt{2}}\right]\left[\left(1+16\Omega^2\right)^{1/2} - 1\right]^{1/2} \tag{21}$$

Assuming linear gas dynamic flow, the stability parameters of the system including combustion process, flow turning, and nozzle were obtained from eqs. 14-16. Figure 8 shows the growth rates of combustion, flow turning, nozzle, and overall growth rate of the system. The contributions of velocity coupling and structural damping were not considered. As shown in Figure 8, because the sum of stability elements is partly negative-partly positive during the burning, this motor became unstable after 0.5 s.

In order to remedy this problem the utilized capabilities are particle damping, adding nozzle cavity, changing the grain configuration, chemical modification of solid propellant which change its response to the pressure variation at various frequencies of the chamber, and active control strategies.

Conclusion

The linear combustion instability for a double base solid propellant has been investigated. The solid rocket motor uses non-metalized double base propellant. The combination of the Lax-Wendroff scheme and the artificial viscosity scheme were implemented to obtain the transient combustion of the solid rocket propellant. Also, the numerical analysis on the characteristics of the interior ballistics has been conducted. The pressure, thrust, specific impulse, and cross flow velocity were obtained for the solid propellant rocket motor. There was a good agreement between the calculated pressure and thrust with simulated ones. Linear contributions of combustion, flow turning, and nozzle were accounted for combustion instability analysis. As a result, the combustion instability was observed after 0.5 s in the solid rocket motor. The applicability of the current work is directed to help motor designers for preventing or eliminating such instability problems in solid rocket motors.

References

1. Avalon G, Ugurtas B, Grisch F, Bresson A (2000) Numerical computations and visualization tests of the flow inside a cold gas simulation with characterization of a parietal vortex shedding. AIAA Paper 2000-3387.
2. Blomshield FS (2001) Historical perspective of combustion instability in motors: case studies. AIAA Paper 2001-3875.
3. Flandro GA, Jacobs HR (1973) Vortex generated sound in cavities. AIAA Paper 1973-1014.
4. Fabignon Y, Dupays J, Avalon G, Vuillot F, Lupoglazoff N, et al. (2003) Instabilities and pressure oscillations in solid rocket motors. Aerospace & Technol 7: 191-200.
5. Flandro GA (1995) On flow turning. AIAA J.
6. Kubota N (2002) Propellants and explosives: Thermodynamical aspects of combustion. Wiley-VCH.
7. Cai W, Ma F, Yang V (2003) Two-Phase Vorticoacoustic Flow Interactions in Solid-Propellant Rocket Motors. J Propulsion Power 1: 19-28.
8. Thomas HD, Flandro GA, Flanagan SN (1995) Effects of Vorticity on Particle Damping. AIAA Paper 1995-2736.
9. Temkin S (2000) Attenuation and dispersion of sound in dilute suspensions of spherical particles J Acoust Soc Am 108: 126-146.
10. Golafshani M, Farshchi M, Ghassemi H (2002) Effects of Grain Geometry on Pulse-Triggered Combustion Instability in Rocket Motors. J propulsion power 18: 123-130.
11. Tseng IS, Yang V (1994) Combustion of a Double-Base Homogeneous Propellant in a Rocket Motor. Combustion & flame 96: 325-342.
12. Terzic J, Zecevic B, Serdarevic-kadic S, Catovic A, Baskarad M (2012) Research of influence of nozzle geometry on internal ballistics performances of solid propellant rocket motors using numerical simulations. Proceedings of 15th Seminar “New Trends in Research of Energetic Materials”, Part II, Czech Republic.
13. Terzic J, Zecevic B, Baskarad M, Catovic A, Serdarevic-kadic S (2010) Prediction of internal ballistic parameters of solid propellant rocket motors. Proceedings of VIIIth international armament conference, Scientific aspects of armament and safety technology, Pultusk, Poland.
14. Lenoir JM, Robillard G (1957) A Mathematical Model to Predict Effects of Erosive Burning in Solid Propellant Rockets. Proceedings of the 6th International Symposium on Combustion, Reinhold, New York 6: 663-667.
15. Willcox MA, Brewster MQ, Tang KC, Stewart DS, Kuznetsov I, et al. (2007) Solid Rocket Motor Internal Ballistics Simulation Using Three-Dimensional Grain Burnback. J Propulsion & Power 23: 575-584.